Heterogeneous photocatalytic degradation of 4-chlorophenol by immobilization of cobalt tetrasulphophthalocyanine onto MCM-41

Azadeh Ebrahimian Pirbazari[*,**,†] **and Mohammad Ali Zanjanchi**[**]

*Faculty of Fouman, College of Engineering, University of Tehran, P. O. Box 43515-1155, Fouman 43516-66456, Iran
**Department of Chemistry, Faculty of Science, University of Guilan, P. O. Box 1914, Rasht 41335, Iran

Abstract−The photocatalytic activity of cobalt tetrasulphophthalocyanine immobilized onto MCM-41 was investigated for photocatalytic degradation of 4-chlorophenol (4-CP) in aqueous solutions. Immobilization of cobalt tetrasulphophthalocyanine complex to the walls of MCM-41 was performed by pre-anchorage of 3-(aminopropyl)-triethoxysilane (APTES) onto MCM-41 *via* post-synthesis method. X-ray diffraction, nitrogen physisorption, diffuse reflectance spectroscopy, energy-dispersive X-ray and FT-IR methods were used to characterize the product. Photocatalytic efficiency of the prepared photocatalyst for degradation of 4-CP was tested under illumination of UV-A and visible light. The reaction intermediates were identified by gas chromatography-mass spectrometry (GC-MS) technique.

Keywords: Phthalocyanine, MCM-41, Immobilization, 4-Chlorophenol, Photocatalytic Degradation

INTRODUCTION

In recent years, global attention has been focused on the removal of hazardous materials from wastewaters [1,2], but a large number of contaminants are resistant to conventional treatment methods. Generally, the traditional methods of treatment may be non-destructive [3], slow at higher concentration [4] or rather ineffective at low contaminant levels. It is therefore crucial to develop newer technologies. Advanced oxidation processes (AOPs) have been successful in degrading most of the organic compounds present in polluted water. The reason for the use of AOPs is due to the inability of biological processes to treat highly contaminated and toxic water. In AOP, the hydroxyl radicals (OH*) are generated in solution and these are responsible for the oxidation and mineralization of the organic pollutants to water and carbon dioxide. In recent years, various advanced oxidation processes, which produce hydroxyl radicals, such as O_3/UV, O_3/H_2O_2, UV/H_2O_2 and Fenton reagent [H_2O_2/Fe(II)], have been applied in wastewater treatment [5]. For over two decades, heterogeneous photocatalytic AOP has been at the forefront of vigorous research activity due to its efficiency of total destruction of pollutants, non-selectivity and formation of kindly products [6].

Heterogeneous photocatalytic systems are mainly based on semiconductor metal oxides since these solids are extremely robust materials and do not become self-degraded [7-10]. However, the performance of some inorganic semiconductors, such as TiO_2, may be far from optimum because their absorption band is deep in the UV region and the absorptivity for visible light is very low. To overcome this limitation a line of research has been aimed at the preparation of doped semiconductors in which the introduction of new electronic states in the semiconductor band gap increases their absorption in the visible [11-14]. Even in cases in which a dopant is introduced, the photocatalytic activity of the resulting semiconductor may still need improvement [15]. Metallophthalocyanine complexes may also exhibit photocatalytic activity towards the degradation of pollutants in liquid phase [16]. However, while the initial activity of metallophthalocyanine-based photocatalysts can be high, their main problem is their poor photostability. Inspired by natural photosynthetic systems, in which metallic porphyrins incorporated in photosynthetic enzymes act as efficient and durable photocatalysts [17,18], we have developed hybrid organic-inorganic photocatalytic systems in which there is encapsulation of a photochemically active organic species, cobalt tetrasulphophthalocyanine (CoPcTs) inside the pores of MCM-41 and we tested for 4-chlorophenol degradation.

Chlorophenols are used in the wood preservation industry, serving as intermediates in the production of pesticides and as additives to inhibit microbial growth in a wide array of products such as adhesives, oils, textiles, and pharmaceutical products. They are released into the environment through various human activities such as pulping industries, chemical industries and also are found in industrial wastewaters, soils, surface waters and ground waters. They constitute a group of serious environmental pollutants that must be eliminated [19].

Herein, we report anchorage of CoPcTs with the aid of 3-(aminopropyl)-triethoxysilane (APTES) to the wall of MCM-41 by post-synthesis method. The resulting solid product was characterized and was tested for photocatalytic degradation of 4-chlorophenol (4-CP). The reaction intermediates were also identified by GC-MS technique.

EXPERIMENTAL

1. Materials and Reagents

Cobalt tetrasulphophthalocyanine complex (CoPcTs) was synthesized, purified and characterized according to the method of Weber and Bush [20]. The MCM-41 was synthesized by our common room

temperature synthesis method [21]. We used tetraethlyleortheosilicate (TEOS, Merck, 800658) as a source of silicon and cetyltrimethylammonium bromide (CTMABr, Merck, 1.02342) as template for preparation of MCM-41 materials. The procedure for the synthesis is as follows. 2.9 g ethylamine (EA) was added to 45 mL of deionized water and the mixture was stirred at room temperature for 10 min. Then, 1.58 g of CTMABr was gradually added to the above solution under stirring within 30 min. After further stirring for 30 min a clear solution was obtained. Then, 4.57 mL of TEOS solution was added dropwise to the solution. The final molar composition of the reacting mixture was as follows:

$$1.0 \ SiO_2 : 1.66 \ EA : 0.215 \ CTMABr : 125 \ H_2O$$

The pH of the reacting mixture was adjusted to 8.5 by slow addition of hydrochloric acid solution (1 M) to the mixture. At this stage, the precipitate is formed. After 2 h under slow stirring, the precipitate was separated and washed by centrifugation. The sample was dried at 45 °C for 12 h.

High-purity 4-CP (Merck No. 802254) was used as a probe molecule for photocatalytic tests. 3-(aminopropyl)-triethoxysilane (APTES) (Merck No. 821619) was used as functionalization agent. Dry toluene (Fluka.No. 89680) and dichloromethane (Merck No. 1.06050) were used as solvents for functionalization reaction. H_2O_2 (Merck No. 1.08597) was used as accelerating oxidant in photocatalytic process.

2. Functionalization of MCM-41 and Photocatalyst Preparation

In a typical reaction, 1.6 g of APTES was added dropwise to a suspension of 1.0 g calcined MCM-41 in 50 mL dry toluene. The mixture was stirred at 60 °C for 1 h. The white solid material was separated by filtration, washed with dichloromethane and dried at 80 °C for 2 h [22]. This compound is called NH_2-MCM-41. Anchorage of the phthalocyanine complex, CoPcTs, to the functionalized support was based on previously reported procedure [23] but modified for a CoPcTs in an aqueous solution. 0.1 g of NH_2-MCM-41 was added to 25 mL CoPcTs 10^{-3} mol/L and pH was adjusted to 3. Then the suspension was stirred for 30 min at room temperature, followed by filtration and washing by distilled water. Finally, the solid product was dried at 100 °C for 5 h. CoPcTs-NH_2-MCM-41 stands for this sample.

3. Characterization

X-ray diffraction (XRD) measurements were performed on a Philips PW1840 diffractometer with Cu-K$_\alpha$ radiation (40 kV, 35 mA), scan rate 0.02° 2θ/s within a range of 2θ of 1-10°. XRD patterns were recorded using an automatic divergence slit system. Diffuse reflectance spectra were recorded by a UV-2100 Shimadzu spectrophotometer, equipped with an integrating sphere assembly. The spectra were recorded at room temperature against barium sulfate and were plotted in terms of absorbance. Specific surface area based on nitrogen physisorption was measured by Sibata surface area apparatus 1100. The samples were degassed at 250 °C for 2 h prior to the sorption measurement. Fourier-transform infrared (FT-IR) spectra were recorded with Shimadzu FT-IR spectrometer (Model 8400). Energy-dispersive X-ray analysis (EDX) joined to XL-30 scanning electron microscope was used for compositional analysis.

4. Photocatalytic Degradation Monitoring

In a typical run, the suspension containing photocatalyst and 50 mL aqueous solution of 4-CP (40 mg/L) was stirred first in the dark

to establish adsorption/desorption equilibrium. Before light irradiation, H_2O_2 was also added. Irradiation experiments were carried out in a homemade reactor. To avoid thermal effects, our homemade reactor had two fans and the beaker containing 4-CP solution was put in the water bath and also the temperature of water bath was kept constant by adding water. The suspension was magnetically stirred before and during irradiation. UV illumination was done with a 400 W Kr lamp (Osram, Germany). The illumination power of the lamp was mainly in the UV-A region ($\approx$90% of the radiated power was in the UV-A region (400-315 nm) and about 10% in the UV-B region (315-280 nm)). For the visible light illumination, a 100 W tungsten lamp (Pars Shahab Lamp Co., Iran) was used as the irradiation source. At certain time intervals, small aliquots (2 mL) were withdrawn and filtered to remove the photocatalyst particles. These aliquots were used for monitoring the degradation progress and for analyzing the intermediate compounds. A spectrophotometer (Shimadzu UV-2100) was used in its conventional mode for monitoring the degradation progress. The reaction intermediates were identified by GC-MS on an Agilent 190915-433. The samples used for GC-MS spectrometry analysis were prepared according to the following procedure. The reaction suspension was first filtered to remove the solid photocatalyst. Then, the filtrate was acidified to pH 1 followed by extraction with dichloromethane. Following evaporation of dichloromethane to dryness, 10 mL methanol was added to dissolve the residue. Then, 1 mL of concentrated sulfuric acid was added and the combined solution was refluxed for about 3 h. The solution was further extracted with dichloromethane followed by concentrating to about 1 mL under reduced pressure.
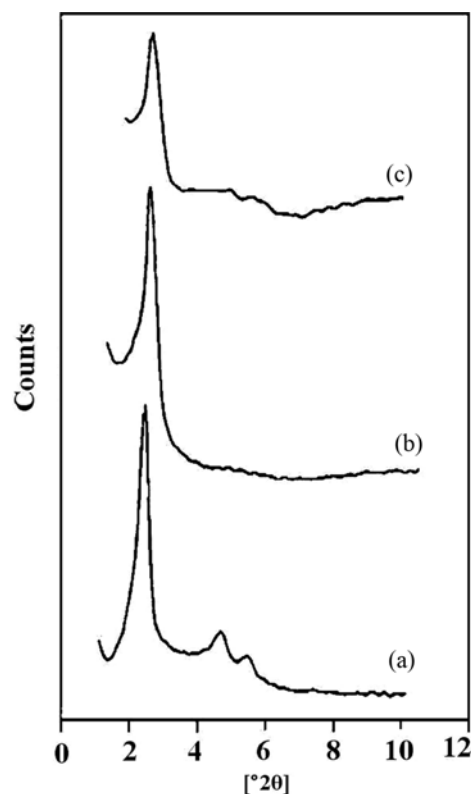

Fig. 1. Powder XRD patterns of (a) calcined MCM-41, (b) NH$_2$-MCM-41 and (c) CoPcTs-NH$_2$-MCM-41.

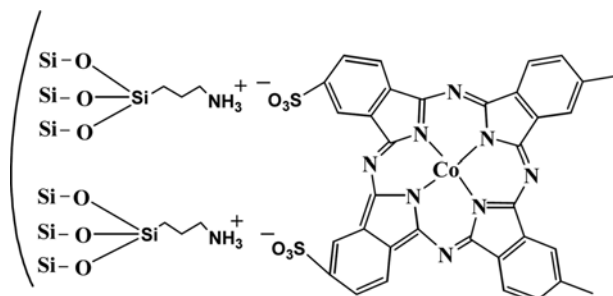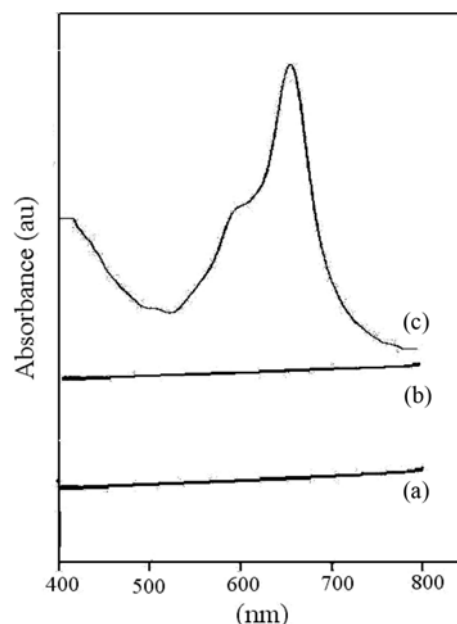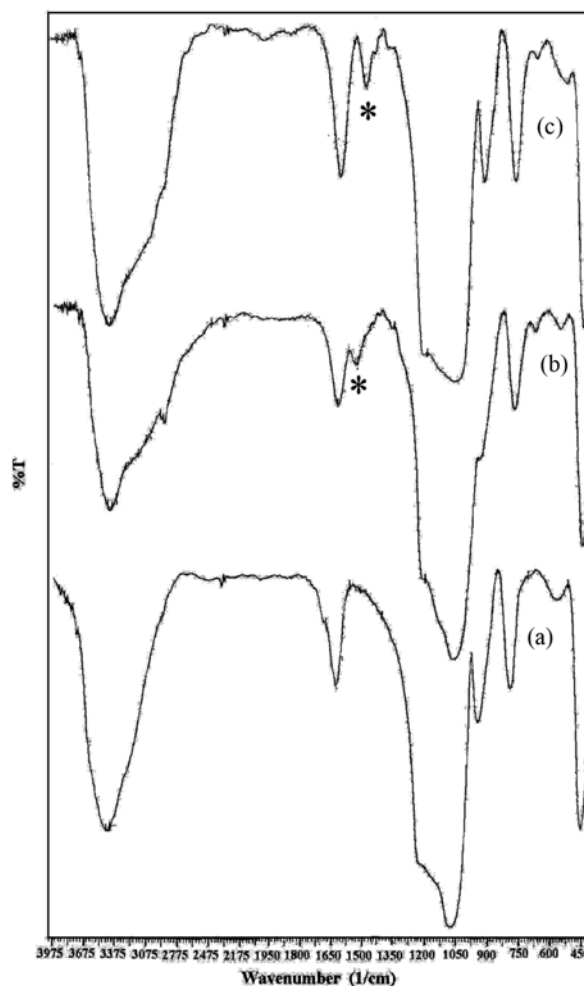**Table 1. Textural parameters and color for the synthesized samples**

Sample	Surface area (m^2/g)	Pore volume (cm^3/g)	Color
MCM-41	1100	0.39	White
NH$_2$-MCM-41	740	0.26	White
CoPcTs-NH$_2$-MCM-41	475	0.17	Pale blue

RESULTS AND DISCUSSION

1. Characterization of the Photocatalyst

The structural features of the MCM-41, modified MCM-41 and photocatalyst were checked by XRD measurements. Fig. 1 shows that the patterns of the modified MCM-41 and photocatalyst are similar to that of the parent MCM-41 sample. However, slight differences in terms of both the positions and intensities of the first (100) peak were observed. Especially in photocatalyst, the reflections are much weaker due to the presence of the guest species (CoPcTs) in the pores and occurrence of some disordering. The decrease in the intensity of reflections, which is well known in immobilization of various catalysts on mesoporous silicas, is attributed to the occupation of mesopore channels [24]. Structural characteristics of the solid materials are listed in Table 1. A decrease of specific surface area from 1,100 m^2/g to 740 m^2/g corresponding to a decrease of the pore volume from 0.39 cm^3/g to 0.26 cm^3/g may indicate a successful anchorage of APTES to the walls of MCM-41. The BET specific surface area of the photocatalyst was evaluated and it was 475 m^2/g. Therefore, there is enough space for oxidizing the organic compounds *via* formation of active species. Fig. 2 shows the interaction of CoPcTs acidic protons with amine groups resulting in the anchorage of CoPcTs to MCM-41. The phthalocyanine content of the photocatalyst was determined by the EDX method. The amount of phthalocyanine loading in the photocatalyst was estimated to be 0.22 mmol/g (1.3% Co).

Diffuse reflectance spectra of the MCM-41, modified MCM-41 and photocatalyst are presented in Fig. 3. The DR spectrum of the photocatalyst (Fig. 3(c)) shows absorption band at 658 nm and shoulder peak at 595 nm corresponding to the monomer and aggregate forms of the CoPcTs, respectively. There is general agreement in the literature that CoPcTs monomer formed in solution shows an absorption maximum at 650 nm, whereas dimeric form exhibits a band in the region of 600-620 nm [25]. The fixation of active catalyst onto appropriate supports is highly desirable to provide high

Fig. 3. Diffuse reflectance spectra of (a) calcined MCM-41, (b) NH$_2$-MCM-41 and (c) CoPcTs-NH$_2$-MCM-41.

Fig. 2. The interaction of CoPcTs acidic protons with amine groups of NH$_2$-MCM-41.

Fig. 4. FT-IR spectra of (a) calcined MCM-41, (b) NH$_2$-MCM-41 and (c) CoPcTs-NH$_2$-MCM-41. The band assigned to amine group is indicated by asterisks.

catalyst stability as well as facile recovery and recycling. Another reason for immobilization of the complexes is to facilitate formation of the more catalytically active species. In fact, these complexes often produce several species including monomers and dimers in solutions while only some species, are more active [26]. In our synthesized photocatalyst almost more than half of the CoPcTs is in the monomeric state (Fig. 3(c)).

The FT-IR spectra of the calcined, modified and the photocatalyst samples are presented in Fig. 4. The spectrum of NH$_2$-MCM-41 (Fig. 4(b)) shows a band at ~1,600 cm^{-1} which is due to the amino groups of APTES anchored to the walls of MCM-41. This band shifts to lower frequency in CoPcTs-NH$_2$-MCM-41 (Fig. 4(c)) where the metal complex is loaded. Liu et al. [27] have assigned the band at 1,634 cm^{-1} to the bending frequency of amino group in the IR spectra of their ruthenium porphyrine encapsulated in an APTES-modified MCM-41. These observations clearly provide more evidences that MCM-41 has been modified by APTES and CoPcTs is anchored to the functionalized MCM-41.

2. Photocatalytic Degradation of 4-CP

Fig. 5 shows the concentration changes of 4-CP with time under various conditions and in the presence of optimum dose of photocatalyst and H$_2$O$_2$ concentration, respectively. Controlled experimental conditions indicate that the light and photocatalyst are essential for efficient degradation of 4-CP in the irradiated aqueous solution, which was hardly degraded in the dark even in the presence of H$_2$O$_2$ and the photocatalyst (Fig. 5(b)). The concentration of 4-CP in the solution decreases with irradiation time when both the photocatalyst and hydrogen peroxide are present. However, the degradation is more rapid when UV irradiation is used instead of visible light. Of course, our UV source provides a UV-A region irradiation, so there is not an enormous difference between the results obtained by the two UV-A and tungsten sources (Fig. 5(e) and (f)). In the experiment under UV irradiation but in the absence of hydrogen
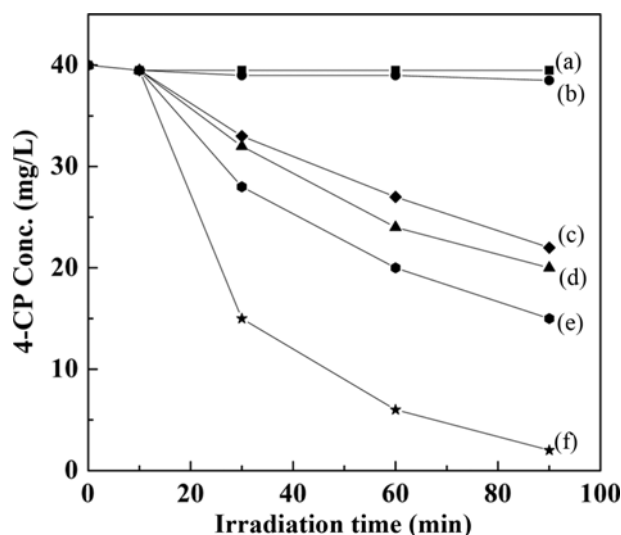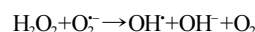
peroxide, the degradation of chlorophenols was much lower than that observed in presence of H$_2$O$_2$ as shown in Fig. 5(d) and (f). Almost complete mineralization is possible within 90 min using hydrogen peroxide besides the photocatalyst under UV radiation for 4-CP. Lack of the photocatalyst in a degradation experiment established in presence of sole H$_2$O$_2$ under UV irradiation converted only half of the amount of chlorophenols (Fig. 5(c)). This shows that a phthalocyanine sensitized photocatalysis reaction is really involved. According to the mechanism of photosensitization reaction, the superoxide radicals are generated *via* energy transfer or electron transfer from an electronically excited photosensitizer to the ground-state molecular oxygen [26]. These species will oxidize 4-CP molecules that are in close contact with them inside the pores. However, the main cause of the elimination of 4-CP may be assigned to the hydroxyl radicals that arose due to the presence of hydrogen peroxide in the solution. Hydrogen peroxide could react with superoxide radicals to generate hydroxyl radicals which are required for photo-mineralization of the organic substrate.

$$H_2O_2 + O_2^{-} \longrightarrow OH^{\cdot} + OH^{-} + O_2$$

The hydroxyl radicals formed during this mechanism are responsible for the oxidation of the chlorophenols, yielding some intermediate compounds and mineralization products. The hydroxyl radical formation was checked using a procedure proposed by Gao et al. [28,29], based on Nash's method [30]. It is based on the quantification of the formaldehyde concentration formed during the oxidation of methanol by the hydroxyl radicals generated in the course of the photocatalytic process. We noticed that the presence of hydroxyl radicals would produce a yellow color owing to the synthesis of diacetyldihydrolutidin [30]. We did not observe this color when H$_2$O$_2$ in presence of the radiation was examined. We observed the color when our photocatalyst, H$_2$O$_2$ and the radiation were employed. The intensity of the color increased with increasing the time of radiation. Since formation of the hydroxyl radicals depends on the presence of superoxide radicals [29], therefore, this experiment may suggest that the superoxide radicals are involved. Hydrogen peroxide could react with superoxide radicals to generate hydroxyl radicals which are required for photo-mineralization of the organic substrate.

3. Identification of 4-CP Degradation Products

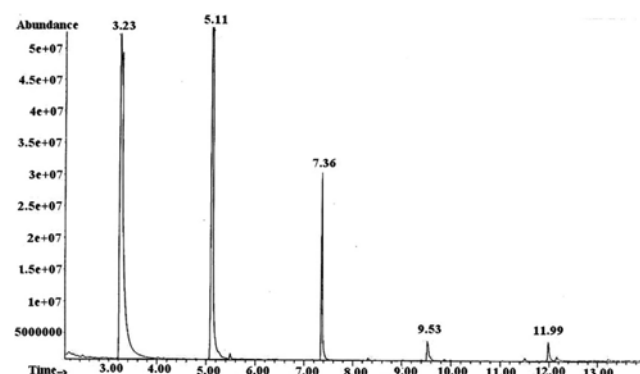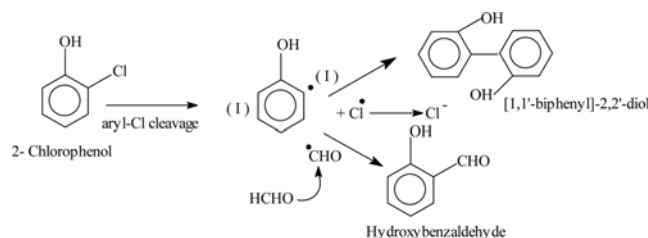To obtain information about intermediates species formed dur-

Fig. 5. Concentration changes of 4-CP at various conditions: (a) photocatalyst+dark, (b) photocatalyst+H$_2$O$_2$+dark, (c) H$_2$O$_2$ +UV-A irradiation, (d) photocatalyst+UV-A irradiation, (e) photocatalyst+H$_2$O$_2$+visible light. and (f) photocatalyst +H$_2$O$_2$+UV-A irradiation, 50 mL 4-CP 40 mg/L, 50 mg catalyst, H$_2$O$_2$ 0.05 mol/L, and pH 5.
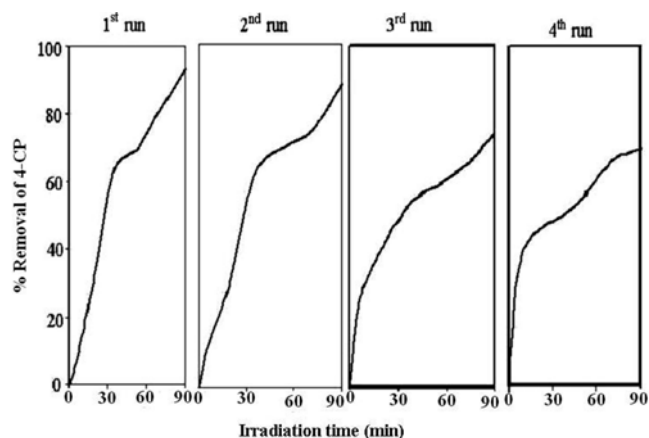
Fig. 6. Gas chromatogram of photodegradation of 4-CP. 50 mL 4-CP 40 mg/L, 50 mg catalyst, 0.05 mol/L H$_2$O$_2$ and 90 min UV-A irradiation.

Table 2. The main intermediates of 4-CP degradation identified by GC/MS

Retention time (min)	Identified intermediate	Molecular structure
3.23	Methyl pyruvate	$H_3CCOCOOCH_3$
5.11	Methyl oxalate	$H_3COOCCOOCH_3$
7.36	Dimethyl malonate	$H_3COOCCH_2COOCH_3$
9.53	Methyl levulinate	$H_3CCOCH_2CH_2COOCH_3$
11.99	Benzoic acid, methyl ester	$C_6H_5COOCH_3$

ing 4-CP degradation process, GC-MS technique was employed. Fig. 6 and Table 2 give major reaction intermediates containing carboxylic acid functional species. Presence of these intermediates can illustrate OH radicals role for degradation of 4-CP. The hydroxyl radicals attack 4-CP, converting them to chlorocatechol and then to chlorobenzoquinone. Subsequently, hydroxyl groups break the aromatic rings of chlorobenzoquinone, transferring them into simple acids like oxalic acid and acetic acid as the final products [31-33]. Chaliha and et al. [32] and Bian and et al. [33] identified the main ring-opened products resulting from 4-CP degradation by GC-MS and discussed the formation mechanism of them. In the proposed mechanism by Chaliha and et al. [32], an electrophilic OH radical adds onto the 4-CP ring at an ortho- or para-position, leading to the formation of chlorocatechol and hydroquinone. On further oxidation, chlorocatechol is likely to be converted to aliphatic acids and hydroquinone to p-benzoquinone, which is easily oxidized to the corresponding dicarboxylic acid, 2,5-dioxo-3-hexenedioic acid. This acid produces maleic acid, which decomposes to oxalic acid, formic acid, acrylic acid, malonic acid and acetic acid. If there are no additional radical competitors in the solution, these low molecular weight organic acids can gradually be mineralized to carbon dioxide, the ultimate oxidation product. Also, a number of the intermediates identified by us (Table 2) are in agreement with those reported in a work on the photodegradation of 2,4-DCP by polydivinylbenzene-supported zinc phthalocyanine [34]. A possible mechanistic pathway illustrating the formation of higher carbon intermediates (benzoic acid in this work) is given in Fig. 7, according to the Rao and et al. report [35]. In the first step, 2-CP molecule undergoes homolytic cleavage of aryl-Cl bond giving rise to radical I and a chloride radical (Cl˙). Alternatively, the dechlorination of 2-CP may result through its interaction with trapped electrons on the semiconductor surface releasing radical I and chloride ions [36]. In a second step, radical I may dimerize to yield [1,1'-biphenyl]-2,2'-diol or combine with formyl radical produced in-situ to give 4-hydroxybenzaldehyde. The observation that formaldehyde is formed

Fig. 7. Rao proposed mechanism of formation of higher carbon intermediates [35].

Fig. 8. Reuse of the CoPcTs-NH$_2$-MCM-41 for 4-CP degradation for four successive cycles.

during the photocatalytic degradation of 2-CP supports this hypothesis. The formation of such higher carbon intermediates lends support for involvement of radicals, e.g., radical I. This result suggests that abstraction of ring-bound chlorine and ensuing free radical reactions such as dimerization and substitution may also take place during photocatalytic degradation of 2-CP. Hydroxyl radicals are known to attack preferentially the aromatic moiety due to their electrophilic nature [37]. As mentioned above, we think in our system that benzoic acid formed by oxidation of hydroxybenzaldehyde. In addition to identifying the organic intermediates, chloride ion was also detected and was determined as the final product of the photocatalysis reaction. Progress of the reaction was evaluated by $AgNO_3$ test method. The presence of Cl in the reaction media accounts up almost 100% for 4-CP degradation if compared to the maximum achievable concentration.

4. Photocatalyst Reuse

The stability of the anchored photocatalysts is very important for its application in environmental technology. Therefore, the effectiveness of photocatalyst reuse was examined for degradation of 4-CP during a four cycle experiment. Each experiment was carried out under identical conditions (Fig. 8). 50 mL 4-CP with an initial concentration of 40 mg/L, 50 mg photocatalyst and 0.05 mol/L H_2O_2 and 90 min irradiation time under UV-A irradiation were used. After each experiment, the solution residue from the photocatalytic degradation was filtered, washed and the solid was dried. The dried photocatalyst samples were used again for the degradation of 4-CP, employing similar experimental conditions. Recycling experiments showed a photocatalytic activity reduction from 93% to 70% of 4-CP degradation after four catalytic cycles. Possibly, deactivation of the part of the catalyst surface, due to permanent adsorption of intermediate species, might be involved in reduction of its activity. In fact, the catalyst surface had a color change from pale blue to pale green after the first photoreaction. Other possibility for the reduction of the activity of the catalyst could be due to probable attack of OH radicals to the anchored phthalocyanine complex.

CONCLUSION

The anchorage of CoPcTs complex in the pores of the functionalized MCM-41 molecular sieves has been achieved by post-syn-

thesis method. The photocatalyst displays an efficient photoactivity for the degradation and mineralization of 4-CP in the presence of H_2O_2 under visible or UV-A illumination. Hydroxyl radicals were probably the main species generated and are responsible for the photodegradation of chlorophenols in our reaction system. Identified intermediate compounds are in agreement with this fact of OH radical involvement in oxidative destruction of 4-CP.

ACKNOWLEDGEMENT

REFERENCES

1. K. Orloff and H. Falk, *Int. J. Hyg. Environ. Health*, **206**, 291 (2003).
2. Mc. Pera-Titus, V. Garcia-Molina, M. A. Baños, J. Gimenez and S. Esplugas, *Appl. Catal. B: Environ.*, **47**, 219 (2004).
3. B. F. Abramovic, V. B. Anderluh, A. S. Topalov and F. F. Gaal, *APT-EFF*, **35**, 1 (2004).
4. E. Pelizzetti, V. Maurino, C. Minero, V. Carlin, E. Pramauro, O. Zerbinati and M. L. Tosato, *Environ. Sci. Technol.*, **24**, 1559 (1990).
5. M. Y. Ghaly, G. Hàrtel, R. Mayer and R. Haseneder, *Waste Manage.*, **21**, 41 (2001).
6. U. I. Gayaa, A. H. Abdullah, Z. Zainala and M. Z. Hussein, *J. Hazard. Mater.*, **168**, 57 (2009).
7. N. Serpone and E. E. Pelizzetti, Photocatalysis, Fundamentals and Applications (1989).
8. M. A. Fox and M. T. Dulay, *Chem. Rev.*, **93**, 341 (1993).
9. D. F. Ollis and H. Al-Ekabi, *Photocatalytic Purification and Treatment of Water and Air*, Elsevier, Amsterdam (1993).
10. D. Bahnemann, J. Cunningham, M. A. Fox, E. Pelizzetti, P. Pichat and N. Serpone, *Aqua. Surf. Photochem.*, 261 (1994).
11. S. Sakthivel and H. Kisch, *Chem. Phys. Chem.*, **4**, 487 (2003).
12. H. Kisch and W. Macyk, *Nachricht. Chem.*, **50**, 1078 (2002).
13. H. Kisch and H. Weiss, *Adv. Funct. Mater.*, **12**, 483 (2002).
14. H. Kisch and W. Macyk, *Chem. Phys. Chem.*, **3**, 399 (2002).
15. M. Alvaro, E. Carbonell, M. Esplá and H. Garcia, *Appl. Catal. B: Environ.*, **57**, 37 (2005).
16. K. Ozoemena, N. Kuznetsova and T. Nyokong, *J. Mol. Catal. A: Chem.*, **176**, 29 (2001).
17. L. Sun, J. Von Gersdorff, J. Sobek and H. Kurreck, *Tetrahedron*, **51**, 3535 (1995).
18. A. Harriman, *Energy Resour. Photochem. Catal.*, 163 (1983).
19. M. Czaplicka, *Science of the Total Environ.*, **322**, 21 (2004).
20. J. H. Weber and D. H. Bush, *Inorg. Chem.*, **4**, 469 (1965).
21. M. A. Zanjanchi and Sh. Asgari, *Solid State Ionics*, **171**, 277 (2004).
22. K. Moller and T. Bein, *Chem. Mater.*, **10**, 2950 (1998).
23. M. Pirouzmand, M. M. Amini and N. Safari, *J. Colloid Interface Sci.*, **319**, 199 (2008).
24. S. Ernst and M. Selle, *Micropor. Mesopore. Mater*, **27**, 355 (1999).
25. K.-Y. Law, *Chem. Rev.*, **93**, 449 (1993).
26. K. Ozoemena, N. Kuznetsova and T. Nyokong, *J. Photochem. Photobiol. A*, **39**, 217 (2001).
27. C. J. Liu, S. G. Li, W. Q. Pang and C. M. Che, *Chem. Commun.*, 65 (1997).
28. R. Gao, J. Stark, D. W. Bahnemann and J. Rabani, *J. Photochem. Photobiol. A: Chem.*, **148**, 387 (2002).
29. A. E. H. Machado, M. D. Franca, V. Velani, G. A. Magnino, H. M. M. Velani, F. S. Freitas, P. S. Muller Jr., C. Sattler and M. Schmucker, *Int. J. Photoenergy*, 1 (2008).
30. T. Nash, *Biochem. J.*, **55**, 416 (1953).
31. S. Chaliha and K. G. Bhattacharyya, *Catal. Today*, **141**, 225 (2009).
32. S. Chaliha, K. G. Bhattacharyya and P. Paul, *Clean*, **36**, 448 (2008).
33. W. Bian, X. Song, D. Liu, J. Zhang and X. Chen, *J. Hazard. Mater.*, **192**, 1330 (2011).
34. L. Wu, A. Li, G. Gao, Zh. Fei, Sh. Xu and Q. Zhang, *J. Mol. Catal. A*, **269**, 183 (2007).
35. N. N. Rao, A. K. Dubey, S. Mohanty, P. Khare, R. Jain and S. N. Kaul, *J. Hazard. Mater.*, **B101**, 301 (2003).
36. K. Konstantinou, V. A. Sakkas and T. A. Albanis, *Appl. Catal. B: Environ.*, **34**, 227 (2001).
37. N. Serpone, D. Lawless, R. Terzian and D. Meisel, in: R. A. Mackay, J. Texter (Eds.), *Electrochemistry in Colloids and Dispersions*, VCH, New York, NY, 399 (1992).